



Hourly composition of gas and particle phase pollutants at a central urban background site in Milan, Italy



A. Bigi^a, F. Bianchi^{b,c}, G. De Gennaro^d, A. Di Gilio^{d,1}, P. Fermo^e, G. Ghermandi^a, A.S.H. Prévôt^b, M. Urbani^{e,2}, G. Valli^f, R. Vecchi^f, A. Piazzalunga^{g,*}

^aDepartment of Engineering "Enzo Ferrari", Università degli studi di Modena e Reggio Emilia, Modena, Italy

^bLaboratory of Atmospheric Chemistry, Paul Scherrer Institute, Villigen, Switzerland

^cDepartment of Physics, University of Helsinki, Helsinki, Finland

^dDepartment of Chemistry, Università degli studi di Bari, Bari, Italy

^eDepartment of Chemistry, Università degli studi di Milano, Milan, Italy

^fDepartment of Physics, Università degli studi di Milano, Milan, Italy

^gDepartment of Environmental Sciences, Università degli studi di Milano Bicocca, Milan, Italy

ARTICLE INFO

Article history:

Received 3 March 2016

Received in revised form 25 October 2016

Accepted 31 October 2016

Available online 19 November 2016

Keywords:

PM_{2.5}

Hourly ionic composition

Gas-phase pollutants

Po valley

ABSTRACT

A comprehensive range of gas and particle phase pollutants were sampled at 1-hour time resolution in urban background Milan during summer 2012. Measurements include several soluble inorganic aerosols (Cl⁻, NO₂⁻, NO₃⁻, SO₄²⁻, Ca²⁺, K⁺, Mg²⁺, Na⁺, NH₄⁺) and gases (HCl, HNO₂, HNO₃, NH₃, NO, NO₂, O₃, SO₂), organic, elemental and black carbon and meteorological parameters. Analysis methods used include mean diurnal pattern on weekdays and Sundays, pollution roses, bivariate polar plots and statistical models using backtrajectories. Results show how nitrous acid (HONO) was mainly formed heterogeneously at nighttime, with a dependence of its formation rate on NO₂ consistent with observations during the last HONO campaign in Milan in summer 1998, although since 1998 a drop in HONO levels occurred following to the decrease of its precursors. Nitrate showed two main formation mechanisms: one occurring through N₂O₅ at nighttime and leading to nitrate formation onto existing particles; another occurring both daytime and nighttime following the homogeneous reaction of ammonia gas with nitric acid gas. Air masses reaching Milan influenced nitrate formation depending on their content in ammonia and the timing of arrival. Notwithstanding the low level of SO₂ in Milan, its peaks were associated to point source emissions in the Po valley or shipping and power plant emissions SW of Milan, beyond the Apennines. A distinctive pattern for HCl was observed, featured by an afternoon peak and a morning minimum, and best correlated to atmospheric temperature, although it was not possible to identify any specific source. The ratio of primary-dominated organic carbon and elemental carbon on hourly PM_{2.5} resulted 1.7. Black carbon was highly correlated to elemental carbon and the average mass absorption coefficient resulted MAC = 13.8 ± 0.2 m²g⁻¹. It is noteworthy how air quality for a large metropolitan area, in a confined valley and under enduring atmospheric stability, is nonetheless influenced by sources within and outside the valley.

© 2016 Elsevier B.V. All rights reserved.

1. Introduction

The interactions between gaseous and aerosol phase pollutants have long been studied due to their impact on air quality (Penkett et al., 1979; Ravishankara, 1997) and on human health (World Health Organization, 2006). In order to investigate processes leading to

atmospheric pollutants formation and ageing in densely populated areas with large emission load (i.e. hotspots), time resolved composition of both gas and particle phase atmospheric compounds are needed. Po valley (Northern Italy) is one of the most important hotspot regions in Europe (Putaud et al., 2010), with Milan metropolitan area exhibiting one of the poorest air qualities within the valley (Bigi and Ghermandi, 2014).

Very few 1-hour time resolution campaigns were accomplished in Milan urban area. Three noteworthy studies resulted from the Limitation of Oxidant Production/Pianura Padana Produzione di Ozono (LOOP/PIPAPPO) campaign held in May and June 1998 in Milan urban background (Nefel et al., 2002). In one of these

* Corresponding author at: Water and Life Lab, I-24060 Entratico, Italy.
E-mail address: pzzndr77@gmail.com (A. Piazzalunga).

¹ Now at ARPA Puglia, Bari, Italy.

² Now at Chemservice Controlli e Ricerche s.r.l., Novate Milanese, Italy.

studies [Baltensperger et al. \(2002\)](#) analysed data by several continuous instruments sampling aerosol physical properties (number size distribution, volatility, hygroscopicity, mass), aerosol chemical composition (BC_E, nitrate, sulphate) (NH₃, HNO₃). This same study showed the large contribution to airborne particles smaller than 40 nm by primary emissions rich in soot content and the increase in secondary and hygroscopic aerosol for particles larger than 50 nm. The second study within PIPAPO, [Putaud et al. \(2002\)](#) collected samples of size-segregated aerosol with 4- and 7-hour time resolution and analysed them for elemental carbon (EC), organic carbon (OC), particulate organic matter (POM) and major ionic species; their results showed the large contribution (>30%) to PM mass by POM, by ammonium nitrate (29% of PM mass) and ammonium sulphate (22% of PM mass). [Putaud et al. \(2002\)](#) found also a diurnal and weekly pattern for traffic-related pollutants (e.g. EC and resuspended mineral dust), the influence of traffic emissions on nitrate formation and of industrial emissions on sulphate formation. In the third study of PIPAPO [Alicke et al. \(2002\)](#) investigated hydroxyl radical formation by measuring several gas phase pollutants by DOAS (differential optical absorption spectroscopy): HCHO, HONO, NO₂, NO, O₃ and SO₂. Their results identified HCHO as the primary source of OH[•] radicals (up to 40% of total OH[•] on clear days), while photolysis of nitrous acid and of ozone provides similar contribution to atmospheric OH[•] (15–30% of total OH[•] each), with the former compound dominating during early morning and the latter during the afternoon. In addition to the above mentioned studies, the aerosol elemental composition and sources were investigated with hourly resolution in Milan by [D'Alessandro et al. \(2003, 2004\)](#) during wintertime and summertime 2001 evidencing quasi-periodical and episodic pollution sources.

Several sources influence the sampling site: [Bernardoni et al. \(2011\)](#) used positive matrix factorization to apportion 4-hour PM₁₀ measurements and showed the diurnal pattern in the relative contribution by resuspended dust, construction works and industry, which altogether account for 48% to total PM₁₀ in summer. These results were confirmed by the a detailed source apportionment exercise in Milan urban background by [Perrone et al. \(2012\)](#), where three years of daily PM_{2.5} and PM₁₀ samples were analysed. This latter study also showed how 60% of summer daily PM_{2.5} derives from traffic and secondary inorganic ions (sulphate, nitrate and ammonium) and contribution of resuspended dust to summer daily PM_{2.5} is only to 3.8%. Consistently emission inventory for the only municipality of Milan assessed Road Traffic (SNAP 7) to be the main source of NO_x and EC for the city of Milan, SNAP 2 (non-industrial combustion) is the main source of OC and the second most important of NO_x, and SNAP 6 (solvent use) is the main source of NM-VOC. Notwithstanding these studies, in Milan there is no available analysis of simultaneous characterization of atmospheric pollutants in both gas and particle phase sampled at a 1-hour resolution. The present article is based on a thorough analysis of measurements of several gas phase pollutants and main chemical composition of PM_{2.5} sampled at 1-hour time resolution. Formation process of PM_{2.5} in Milan will be presented along with the influence of meteorological conditions and air mass trajectories. Observations include HCl, HONO, HNO₃ and NH₃, i.e. the first published measurement of hydrochloric acid in the Po valley and the first 1-hour resolution measurements of nitrous and nitric acids in the last 15 years in Milan. Details on the instrumentation and methods used are presented in [Section 2](#). Results and conclusions are found in [Sections 3 and 4](#) respectively.

2. Data and methods

Milan (45° 28'N; 9° 13'E) urban area counts about 1,500,000 inhabitants and is the second largest town in Italy, after Rome, and

considering the whole Milan province the population rises up to about 3.1 millions inhabitants.

The data here presented were collected on the roof of the Department of Chemistry, University of Milan, at a ~10 m a.g.l. within the University campus, a site representative of central urban background conditions for the city. Sampling was performed from June 5th until July 23rd 2012.

Hourly resolution composition of PM_{2.5} for soluble inorganic ions composition and for gases was determined using a commercially available Ambient Ion Monitor (AIM) URG-9000D (URG Corp, USA). In particle phase five anions (Cl⁻, F⁻, NO₂⁻, NO₃⁻, SO₄²⁻) and five cations (Ca²⁺, K⁺, Mg²⁺, Na⁺, NH₄⁺) were determined. F⁻, Ca²⁺, K⁺, Mg²⁺ and Na⁺ were often below the detection limit and therefore not analysed in details. The gases determined include hydrochloric acid (HCl), nitrous acid (HONO), nitric acid (HNO₃), ammonia (NH₃) and sulphur dioxide (SO₂). The AIM consists of a sampling system for both gas and particles, coupled with two ion chromatographies for the analytical determination. Gases are collected by a liquid diffusion denuder with H₂O₂ 5 mM running continuously at 10mLh⁻¹ flow rate. Particles are collected in a chamber supersaturated with ultrapure water vapour: water soluble particles are allowed to grow and then inertially separated and injected into the ion chromatographies. Further instrumental details and the calibration procedure used in this study can be found in [Markovic et al. \(2012\)](#). AIM data were compared to off-line daily data from PM_{2.5} samples collected during 22 days throughout the campaign by denuded filter-pack setup ([Vecchi et al., 2009](#)): the system consisted in two dry annular denuders removing both acidic and basic gases, followed by a filter pack made of a quartz fibre front filter and a nylon fibre backup filter. Once the campaign ended, AIM blank values for particle-phase aerosol were estimated by inserting a quartz fibre filter between the denuder and the filter pack over 5 full days.

Comparison of AIM and denuded filter pack showed statistically significant (by ANOVA test) and large coefficients of determination for linear regression models between off- and on-line data for all species (Fig. S1), supporting the reliability of the patterns observed by AIM. Regression coefficients were close to unity for HNO₂ + HNO₃ and NH₃, while some difference occurred between particle-phase compounds, with lower NO₂⁻ + NO₃⁻ levels observed by AIM and lower values for SO₄²⁻ and NH₄⁺ observed by denuded filter-pack. Assuming that the denuded filter pack reported in [Vecchi et al. \(2009\)](#) is artefact-free for nitrogen compounds, some bias likely affects ammonium in AIM measurements, preventing a fully-correct estimate of ion balance for the experimental dataset. Part of the offset between the two measurement sets might also be due to the possibly different transmission efficiency curve between respective size-selective inlets: AIM uses a custom PM_{2.5} cyclone, while denuded filter pack used a US-EPA equivalent PM_{2.5} inlet equipped with a PM₁₀ sampling head and a WINS PM_{2.5} impactor downstream.

Gaseous precursors levels during AIM blank test resulted similar to their respective mean observed during the campaign, indicating an efficient collection of gas and a complete transmission of particles by the denuders. Significant particulate sodium was observed during blanks and ascribed to contamination in the ultrapure water used in the supersaturated chamber during the blank test. The low particulate nitrite, nitrate and ammonium observed during blank testing (i.e. < 1µgm⁻³) can be considered negligible. Slightly larger blank for particulate sulphate was observed (~1.5µgm⁻³), but considered sufficiently low to support the reliability of the AIM measurements for this compound.

Elemental carbon (EC) and organic carbon (OC) measurements were collected by a Model-4 Semi-Continuous ECOC Field Analyser by Sunset Laboratory, USA ([Bae et al., 2004](#)). The carbon analyser was provided with a PM_{2.5} cyclone and operated at a 24L min⁻¹ flow rate. Measurement had 1-hour time resolution, comprising 45 min

for sampling and 15 min for thermal-optical analysis. The analysis followed a high temperature analytical protocol featured by 2 steps in inert atmosphere (625 °C, 870 °C) and 3 steps in oxidizing atmosphere (650 °C, 675 °C, 870 °C). During most of the campaign the split point (i.e. the separation between OC and EC) occurred in inert atmosphere: the pre-combustion of EC was attributed to the low carbon amount and to the presence of undesired oxygen or of metal oxides accumulated on the filter. The data analysis included only EC-OC measurement having a split point above 650 °C (Jung et al., 2011), in accordance with EUSAAR2 protocol for off-line laboratory measurements (Cavalli et al., 2010). Both calibration and filter replacement were performed on a weekly basis; no EC-OC data are available on Sundays.

Aerosol light absorption coefficient (σ_{ap}) was measured by a Multi-Angle Absorption Photometer (MAAP, model 5012, Thermo Scientific Corp., USA) equipped with a PM_{2.5} inlet. Atmospheric equivalent black carbon concentration (BC_E) is estimated by the instrument using a MAC (mass specific absorption cross section) of 6.6m²g⁻¹ (Petzold et al., 2002). BC_E measurements had a 5-min resolution and the data were then averaged to 1 h. To evaluate atmospheric dispersion conditions, ²²²Rn short-lived decay products measurements were performed using the experimental methodology reported in Marazzan et al. (2003). Hourly measurements of meteorological parameters (wind speed and direction, temperature, relative humidity, pressure, global solar radiation and precipitation) were sampled on the roof of the Department of Physics, University of Milan, at ~10 m a.g.l., within the grounds of the University campus. Concentration of NO, NO₂ and O₃ were provided by an urban background station sited 400 m NE of the campus and within the air quality monitoring network of the Regional Environmental Protection Agency of Lombardy (ARPA).

A tentative localization and identification of the pollution sources was performed by four techniques: analysis of conditional bivariate probability function (CBPF), bivariate polar plots, air mass origin by simulated backtrajectory and backtrajectory statistical models (BSMs). The former two techniques are headed to identify local sources, while backtrajectories were used to potentially track pollution events due to distant sources. CBPF technique estimates the probability that a specific concentration range is observed within a given wind sector, depending upon wind speed (more details in Uria-Tellaetxe and Carslaw, 2014). Bivariate polar plots (Carslaw and Ropkins, 2012) are a level plot in polar coordinates where colour scale represents pollutant concentration and polar coordinates are a smoothed interpolation of wind speed and wind direction by generalised additive model (Wood, 2006). Origin of air masses arriving in Milan at 100 m a.g.l. was estimated with 36-hour long backtrajectories simulated by HYSPLIT (Draxler and Rolph, 2013) using 0.5° GDAS meteorological data. 24 trajectories per day were computed, i.e. one per hour. The statistical models applied to backtrajectories include concentration field (CF), potential source contribution function (PSCF) and gridded difference (GD) using respective functions in Carslaw and Ropkins (2012). All of the three attempt to combine trajectory path to concentration at the receptor; further details about BSMs can be found in Carslaw and Ropkins (2012) and Fleming et al. (2012). Scheifinger and Kaiser (2007) proved BSMs to provide useful information on potential source areas only for distances within the mean residence time of the investigated compound; for trajectories longer than this period the effect of turbulent dispersion and removal processes, neglected by the statistical models and the backtrajectories, may lead to unreliable results (Han et al., 2005). In the present study trajectory statistical models were tested for several species, although significant results occurred only for SO₂, SO₄²⁻ and NH₃. For sulphur dioxide Scheifinger and Kaiser (2007) suggest to limit backtrajectories within 60 h: in this study a length of 36 h (i.e. largely within 60 h) was used for all pollutants.

Few different emission inventories were used to review BSM outputs and to identify realistic potential sources: a plot pairing inventory database and corresponding area is presented in Fig. S2. Emission inventories for Lombardy, Piedmont and Veneto were consistently compiled (INEMAR, 2015), resulting in a bottom-up inventory with a spatial resolution at the municipality district level. These inventories are compliant to the EMEP-CORINAIR guidebook, the IPCC guidelines and the Good Practice Guidance, they are classified accordingly to SNAP (Selected Nomenclature for Air Pollution) and the emission data used in this study refers to 2010 for Lombardy and 2008 for Piedmont and Veneto. Emissions for Aosta Valley, Liguria, Rhône Alpes and Provence-Alpes-Côte d'Azur refers to 2008, have a spatial resolution at the municipality district level and include point sources for the three former regions. Data were provided by the project AERA (Air Environnement Regions ALCOTRA) through a Web Map Service (AERA, 2015). Finally, emissions for all other regions involved in this study were provided by the UNECE/EMEP emission inventory for 2012. Accuracy and uncertainty of these inventories are different, as well as the procedure to build them, their spatial resolution and their reference year. In this study inventories were used to identify areas with significant SO₂ emissions (e.g. large industrial plants) and to approximately compare potential sources, therefore the discrepancies between these databases were considered negligible for the purpose of this analysis. Nonetheless the closer the investigated area is to Milan, the more detailed is the inventory used, allowing a reliable analysis of nearby and directly impacting sources.

All statistical data analyses were performed within the software environment R 3.0.2 (R Core Team, 2013). All data are reported in local time, i.e. Central European Summer Time (CEST).

3. Results and discussion

In the following the data will be presented and discussed in specific subsections for each common species, including their pattern, formation and removal processes (if known) and their potential source. The analysis investigates the average concentration pattern over the whole sampling period, and the variability of a subset of pollutants under different atmospheric dispersion conditions.

3.1. Meteorological setting

June and July 2012 were featured by high pressure fields originated by the Azores high and occasionally by subtropical anticyclones (Fig. S3). Large values of mean geopotential height at 500 hPa occurred during the sampling campaign, when June was characterized by anticyclonic curvature and moderately positive anomaly and July by a slightly cyclonic curvature. This meteorological context determined recurrent atmospheric stability, clear-sky and high temperatures, enhancing photochemical activity and formation of tropospheric ozone. Hot weather conditions occurred between the end of June and the beginning of July and, after a short instability period, since July 8th. Main meteorological events reducing atmospheric pollutants levels occurred at the beginning of June prompted by moderately perturbed fluxes and Atlantic cold fronts, on the 14th and 15th of July due to ventilation originated by a temporary positioning in the North of Alps of the maximum of the Azores high, and on July 21st when a cold front led to intense rainstorms in Milan and surroundings. A mountain-valley breeze regime was present during large part of the campaign, with low N winds at night (< 2ms⁻¹), increasing and rotating at daytime until a SW flow is established in the afternoon with speeds up to 4ms⁻¹. These meteorological conditions were typical of summers in Northern Italy, therefore notwithstanding measurements did not

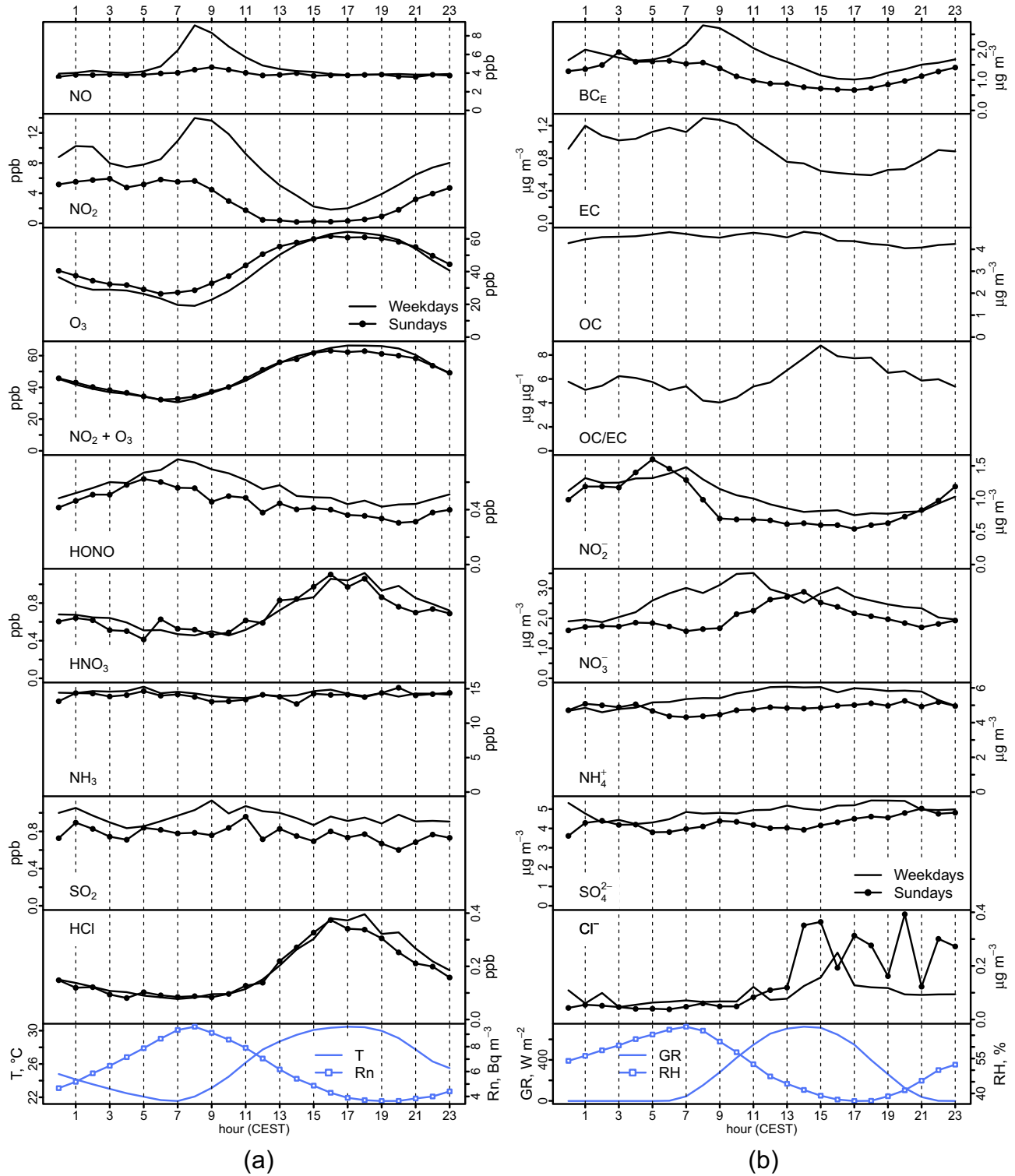


Fig. 1. Diurnal pattern for weekdays and Sundays for several gas phase (panel a) and particle phase (panel b) pollutants. Diurnal pattern of few meteorological variables and parameters are also included: temperature (T), radon concentration (Rn), global radiation (GR) and relative humidity (RH).

cover the whole summer, they are well representative of the entire season. A summary of statistical values for the measured parameters is presented in Table B1. In Fig. 1 the diurnal pattern during weekdays and Sundays are presented for several observed pollutants, along with temperature (T), radon concentration (Rn), global radiation (GR) and relative humidity (RH).

3.2. Nitrogen oxides and ozone

Nitric oxide shows sharp peaks at mornings only on weekdays, indicating a source from rush hour traffic, along with relatively low atmospheric mixing; NO rapidly declines due to vertical mixing and its oxidation to NO₂ by O₃ and by the available radical groups.

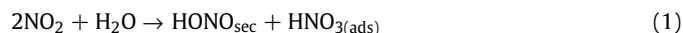
Nitrogen dioxide peaks at morning rush hours. The afternoon decrease in NO₂ is driven by 3 processes: dilution due to the rise in mixing layer height, photolysis to NO under intense solar radiation and reaction with OH[•] to nitric acid. The difference between weekdays and Sundays is noteworthy for both NO and NO₂, strongly indicating an anthropogenic source, most likely traffic, of these compounds.

Ozone shows an afternoon peak generated by the large availability of OH[•] radicals and possibly by the re-entrainment of O₃ within the residual layer (Zhang and Trivikrama Rao, 1999). Indeed the sum of NO₂ and O₃ shows a slightly higher peak on weekdays indicating the small contribution by fresh emissions to oxidant species. Ozone exhibits a very mild weekend effect (Cleveland et al., 1974; Jiménez et al., 2005; Pollack et al., 2012; Tonse et al., 2008; Wang et al., 2014), e.g. higher mixing ratios on Sundays due to lower NO_x emissions over the weekend and therefore reduced titration of O₃, as shown for Milan by Vecchi and Valli (1999). Since 1700 CEST mixing decreases leading to an increase in NO_x and a drop in ozone. Diurnal pattern for NO_x and O₃ are highly similar to mean diurnal pattern for long term measurements in Modena, 160 km SE of Milan, Po valley (Bigi et al., 2012), where ozone exhibits also similar levels to those observed in Milan, consistently with the atmospheric homogeneity across the valley.

3.3. Nitrous acid and nitrites

Gas-phase nitrous acid (HONO) shows a pattern similar to past observations in Milan by Stutz et al. (2002) and Febo et al. (1996), featured by lower mixing ratios at daytime, due to photolysis, and peak at nighttime, most likely by heterogeneous formation. Particle-phase nitrites (NO₂⁻) exhibit a diurnal pattern highly similar to HONO, as observed in Marseille (Acker et al., 2005), suggesting that part of atmospheric HONO is formed heterogeneously onto particle surfaces under high RH conditions. Traffic emissions are another possible source of HONO: Kurtenbach et al. (2001) found large variability in the ratio HONO/NO_x from road tunnel measurements depending on fuel, emission control systems and motor load. A ratio for HONO/NO_x of 1% was used in this study, similarly to the ratio used by Michoud et al. (2014) for Paris and higher than 0.65% as used by Stutz et al. (2002) for Milan. In order to remove HONO direct emissions from total HONO, secondary HONO was estimated as HONO_{sec} = HONO – 0.01 · NO_x, resulting in a ~80% of total HONO from secondary origin.

Main formation mechanism of HONO_{sec} in urban atmosphere is expected to proceed heterogeneously onto surfaces, following reactions (1) and (2), with reaction (1) being the most likely process (Kleffmann, 2007). It is still unclear whether the contribution of heterogeneous formation of HONO_{sec} onto soot particles (Kalberer et al., 1999) is a significant source to atmospheric concentrations (Kleffmann, 2007; Ziemba et al., 2010) or not (Finlayson-Pitts and Pitts, 2000).



Latest published measurements of nitrous acid in Milan urban background were collected in May and June 1998 by Alicke et al. (2002) and Stutz et al. (2002). The latter investigated HONO formation by DOAS-resolved vertical profiles and found that HONO_{sec} was formed at ground. Stutz et al. (2002) estimated that 1 molecule of HONO_{sec} was released each 25–40 molecules of NO₂ and assessed the NO₂ conversion efficiency to be an order of magnitude lower than expected according to reaction (1).

In Alicke et al. (2002) HONO mixing ratios by DOAS exhibited a nighttime and daytime mean of 0.92 ppb and 0.14 ppb respectively.

In summer 2012 the mean mixing ratios observed were of 0.6 ppb at nighttime and 0.5 ppb at daytime, with the latter being largely higher than in 1998 and potentially biased by artefacts. Maximum nitrous acid levels were similar in both studies: 4.4 ppb and 4.2 ppb in 1998 and 2012 respectively.

In order to assess whether a long term trend in HONO is present and 2012 daytime data are artefact-freefall, an analysis of NO₂ levels from 1998 through 2012 was performed. Mean daytime NO₂ concentration during the two sampling campaigns were 18.3 ppb and 4.9 ppb in 1998 and 2012 respectively, while mean nighttime NO₂ concentration was 33.2 ppb in 1998 and 8.8 ppb in 2012. These observations are consistent with an estimated long term trends for deseasonalized monthly mean concentration of NO₂ of $-1.47 \pm 0.17 \text{ ppb year}^{-1}$ (trends are estimated by Generalised Least Squares method as in Bigi and Ghermandi (2014)). Given the large NO₂ concentrations in 1998, Stutz et al. (2002) found a large contribution of direct emissions to atmospheric HONO, notwithstanding they made use of a low HONO/NO_x ratio, i.e. 0.65%. The large decrease in NO₂ from 1998 to 2012 should cause a significant decrease in HONO over the same period, although, according to 2012 HONO data, a decrease occurred only at nighttime. Several intercomparison studies of HONO measurements by DOAS and chemical instruments (e.g. wet denuder and LOPAP) showed how results from different techniques agreed well at nighttime, while HONO by standard wet denuders might suffer from positive artefacts at daytime (Kleffmann et al., 2006); these might occur by reaction on denuder surface either of semivolatile diesel exhausts with NO₂ (Gutzwiller et al., 2002), either of pure NO₂ (Kleffmann et al., 2006), either of NO₂ and S(IV) (Spindler et al., 2003). The high HONO and HONO_{sec}/NO₂ ratio in 2012 at daytime suggest that 2012 daytime HONO mixing ratios might be biased by a chemical interference in the denuder, since are not consistent with the observed decrease in NO₂ from 1998 to 2012 and the corresponding decrease in nighttime HONO over the same period.

Assuming that during nighttime most of nitrous acid is formed through reaction (1), which is first order in NO₂, formation rate between two generic instants t_1 and t_2 was computed according to Eq. (3).

$$\overline{F}_{\text{HONO}_{\text{sec}}} = \frac{[\text{HONO}_{\text{sec}}](t_2) - [\text{HONO}_{\text{sec}}](t_1)}{(t_2 - t_1)[\text{NO}_2]_{\text{night}}} \quad (3)$$

Formation rate is best estimated for nights when NO and NO₂ levels are low, in order to consider negligible both direct HONO emissions by traffic and positive artefacts, and when HONO formation is steady and lasts throughout the night, in order to average over several hours. These conditions are met between June 18th and 19th, since NO and NO₂ concentration were steadily below 5 ppb and 15 ppb (Fig. 2), and lead to a formation rate of 0.009 ppb HONO_{sec}/h (ppb NO₂), consistently with the rate of (0.012 ± 0.005) found by Alicke et al. (2002) in Milan by DOAS.

3.4. Nitric acid, nitrates and ammonia

Nitric acid is formed by reaction of OH[•] with NO₂ leading to HNO₃ characteristic pattern featured by a single afternoon peak, when hydroxyl radicals are abundant. Nitric acid formation is expected to be controlled by the availability of OH[•] rather than by NO₂, since HNO₃ diurnal pattern exhibits no difference between weekdays and Sundays, contrarily to NO₂, whose peak is above 12 ppb on weekdays and ~5 ppb on Sundays.

Atmospheric particle nitrate is expected to be formed by two main pathways, either through reaction of HNO₃ with NH₃ or through absorption of N₂O_{5(g)} (Lammel and Cape, 1996; Finlayson-Pitts and Pitts, 2000): the former reaction is homogeneous, the latter is heterogeneous and occurring only at slow

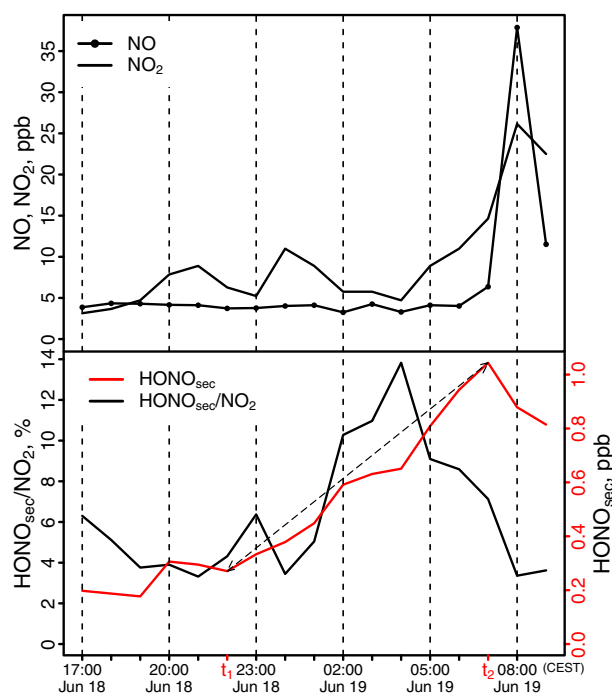


Fig. 2. Formation of HONO_{sec} during the night between June 18th and 19th 2012. The arrows indicate the data used to calculate first-order formation rate.

rates and at nighttime, since N_2O_5 and NO_3 photolyse very rapidly (see Appendix A). The heterogeneous pathway is expected to form significant amount of aerosol nitrate: Alexander et al. (2009) estimated a similar contribution by the two pathways on an annual basis in Italy, while Michalski et al. (2003) estimated the heterogeneous pathway to contribute up to 50% to total summer nitrate in La Jolla (Southern California).

Diurnal pattern of nitrate shows an increase since 0200 to 1000 CEST during weekdays, whereas on Sundays exhibits steady concentration at mornings and an increase since 0900 to 1400 CEST. Afternoon patterns do not differ both in shape and levels between weekdays and Sundays. Two methods were used to investigate partitioning of ammonium nitrate with its precursors at thermodynamic equilibrium: ISORROPIA 2.1 (Fountoukis and Nenes, 2007) simulation model (forward mode and thermodynamically stable state conditions) and dissociation constants for reaction (A.2) of ammonium nitrate aerosol assuming a single-component aerosol (see Appendix B for details and calculations). Both methods show how patterns of atmospheric nitrate and theoretical partitioning do not fully match (Fig. S4), differently to other continental climate sites in summer (e.g. Melpitz, Germany (Poulain et al., 2011)), suggesting that condensation/evaporation processes do not exclusively control aerosol nitrate.

At nighttime N_2O_5 is expected to be partly responsible of the nitrate increase, also suggested by the slower formation rate compared to the one required by the thermodynamic equilibrium of the homogeneous reaction according to ISORROPIA (not shown). The nitrate increase after sunrise is possibly kept up by homogeneous reaction (A.2), triggered by the rapid formation of nitric acid from NO_2 rush hour emissions: since there is no evidence of nitric acid rise until 0900–1000, possibly this early morning HNO_3 is rapidly converted to nitrate. On Sundays nitrate increases from 0900 to 1000, i.e. most likely through the diurnal homogeneous reaction: the lower NO_2 levels over the weekend (Saturday and Sunday) lead to a smaller production of early morning HNO_3 and nighttime N_2O_5 . Nitrate decreases during afternoons due to temperature increase and the

shift of ammonium nitrate equilibrium to the gas-phase. Occasional morning increase in nitrate might be due also to re-entrainment of nitrate within the residual layer, which has been shown to provide a significant contribution to ground level concentration in Milan in summer (Curci et al., 2015).

Diurnal pattern for ammonia shows a steady profile. This is due to several reasons: total $\text{NH}_3 + \text{NH}_4^+$ is mainly in gasphase ammonia, therefore the particulate phase is not significantly affecting NH_3 concentration. Variability in aerosol nitrate diurnal pattern is almost negligible compared to ammonia levels, therefore no significant amount of ammonia is expected to be released in the afternoon when ammonium nitrate equilibrium moves towards gasphase. Besides, in the afternoon HNO_3 increases, leading to ammonium nitrate formation partly compensating the dissociation of ammonium nitrate. Sulphate shows quite constant concentration and no significant change in NH_3 is expected from ammonium sulphate. Finally NH_3 emissions might be slightly larger during daytime, but compensated by dilution from the enhanced boundary layer.

CBPF for nitrate shows how peak concentration of this compound is associated to very low wind speeds, i.e. is formed locally and concentrations increase due to the low dispersion conditions. On the contrary, median to moderate nitrate concentrations are associated to S or SSE winds, i.e. winds associated to moderate–large ammonia content. CBPF for ammonia indicates that larger observed levels are associated to distant sources at S, SSE, E and W of Milan, most likely emissions from agricultural activities in the Po valley surrounding the city. The existence of farther sources of ammonia were investigated also by BSMs (see Fig. S5), which confirm emissions within the Po valley as main responsible for ammonia levels in Milan. This is consistent with 2010 emission inventories, ascribing 97% of all ammonia emissions to agricultural activities, and the remainder to traffic and wastewater treatment (Bigi and Ghermandi, under review).

During the campaign, significant pollution episodes occurred, both for particulate nitrate (June 8th–9th) and ammonia (June 27th–28th). The former occurred during a 48-hour period of relatively low temperature featured by a blocked atmosphere and an elevated inversion (Fig. S6), the latter occurred during a rapid transport of ammonia originated in the Po valley (Fig. S7).

3.5. Hydrochloric acid

Known anthropogenic sources of HCl are coal combustion (Lightowers and Cape, 1988), biomass burning and waste incineration (Kaneyasu et al., 1999), whereas main natural source of HCl is sea-salt (Eldering et al., 1991). Few measurements of atmospheric HCl mixing ratios are reported in the literature and the data here presented are the first published measurements in Milan, to authors knowledge. Mean HCl level during the campaign resulted in 0.19 ppb. In summer 1999 Bari et al. (2003) observed 0.32 ppb and 0.28 ppb of HCl in two areas within New York City and attributed it to sea-salt. Eldering et al. (1991) observed HCl mixing ratios up to 3 ppb in Southern California in summer 1986 and demonstrated its formation by sea-salt chloride depletion by attack of HNO_3 . Kaneyasu et al. (1999) showed the contribution of waste incineration to both atmospheric HCl and aerosol chloride during winter 1991 in the Japanese Kanto Plain, where chloride ranged between $10\mu\text{g}\text{m}^{-3}$ and over $70\mu\text{g}\text{m}^{-3}$. The study by Kaneyasu et al. (1999) showed how HCl emissions combined with NH_3 to $\text{NH}_4\text{Cl}_{(p)}$, which finally dissociate to gaseous HCl and NH_3 at daytime with warmer atmospheric temperatures.

Observed HCl in Milan exhibits no weekly pattern, but a clear diurnal pattern identically repeated throughout the week and best correlated to atmospheric temperature (see Fig. 1). This outcome was confirmed by a bivariate polar plot analysis conditioning concentration on atmospheric temperature instead of wind speed, indicating

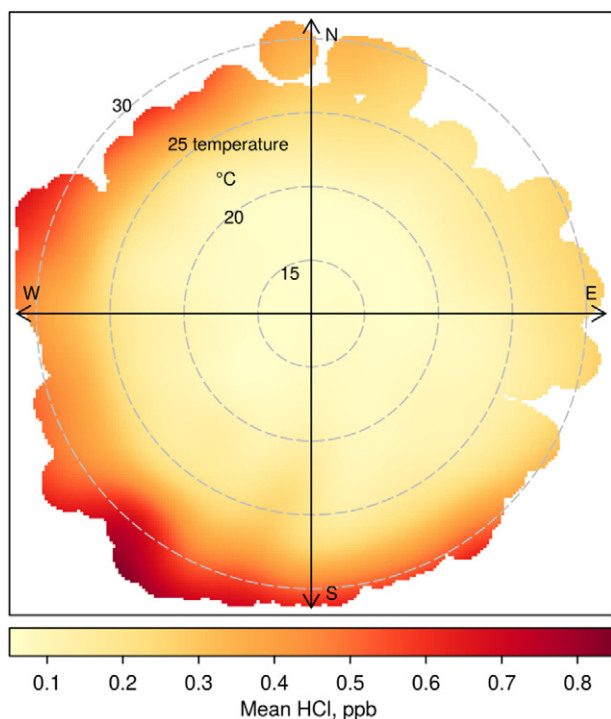


Fig. 3. Bivariate polar plots for hydrochloric acid with atmospheric temperature ($^{\circ}\text{C}$) as radial scale.

that higher HCl values are associated to higher temperature and do not depend on wind direction (Fig. 3). Atmospheric temperature is higher in the afternoons, when a SW breeze is established, explaining why in Fig. 3 larger HCl is associated to SW winds. The presence of a significant distant source (e.g. sea) for HCl was checked by BSMs, which pointed to a near source, excluding long range transport (see Fig. S8). Similarly, the analysis of sodium chloride balance, considering both aerosol and gas phase, resulted in a large excess in Chlorine. These outcomes suggest that HCl is originated by a chlorinated compound free to evaporate in the atmosphere from a non-point source, and sufficiently abundant to generate significant atmospheric HCl levels. Unfortunately available data are not sufficient to explain this excess in Chloride and further samplings are needed to unveil the origin of HCl.

3.6. Sulphur dioxide and sulphates

SO_2 concentration in Milan are similar to other European cities (see Henschel et al., 2013, for an European overview) and its diurnal pattern, along with that of sulphate, shows no distinctive features, besides slightly lower concentrations on Sundays. Few stationary sources of SO_2 have significant emissions and are sufficiently near Milan to directly impact the city: the largest is an industrial area including a refinery and a carbon black manufacture sited 40 km West of the sampling site and emitting altogether $\sim 6900 \text{ Mg year}^{-1}$ of SO_2 (E1 in Fig. 4). Other significant SO_2 sources are as follows: a refinery sited 50 km South-West of the sampling site, with an estimated SO_2 emission of $4500 \text{ Mg year}^{-1}$ (E2 in Fig. 4) and a refinery sited 130 km ESE (annual SO_2 emission of 1600 Mg) (E3 in Fig. 4).

CBPF, bivariate polar plots and trajectory statistical models were used to identify whether any of the above potential source is impacting the sampling site. CBPF analysis associates low SO_2 levels (0.0–0.5 ppb, i.e. below the 20th quantile) to Northerly winds (CBPF plots for SO_2 are in Fig. S9). Moderate SO_2 concentrations (20th–70th quantile) are associated to a Southern source (possibly E1 and/or Genoa) and a Western source (possibly E2). Highest concentrations are associated to a source SW of the site, most likely E1. Consistently bivariate polar plot for SO_2 associates mean levels to W and SW winds (Fig. 5e).

Potential sources of long-range transported SO_2 identified by BSMs were nearby Venice (250 km E of Milan) and in the Ligurian Sea/Ligurian shore (Fig. S10). At the former a large refinery and a power plant are present; at the latter SO_2 emissions are expected by ship traffic and by a power plant (E4 in Fig. 4) which is partly coal fired. Finally some contribution could occur by sources nearby Marseille (E5 in Fig. 4), where an overall SO_2 emissions in the order of $50,000 \text{ Mg year}^{-1}$ is expected.

Regarding sulphate, CBPF associates its lowest concentration to Northerly winds (see Fig. S11), similarly to SO_2 . Low sulphate concentration is associated to low Eastern winds, possibly aged emissions from Venice or E3. Median sulphate levels (SO_4^{2-} ranging between 4.1 and $5.4 \mu\text{g m}^{-3}$, i.e. between 40th and 60th quantile) are associated to moderate SW winds, suggesting a distant origin, eventually E4. Peaks in sulphate are associated to low SW winds and possibly originate from E1 emissions. Backtrajectories models for sulphate suggest possible sources similar to SO_2 (Fig. S12): all three statistical models indicate a source in the Ligurian sea, most likely maritime traffic and E4, a source nearby Venice and possibly some contribution from the area of Marseille. BSMs results consider

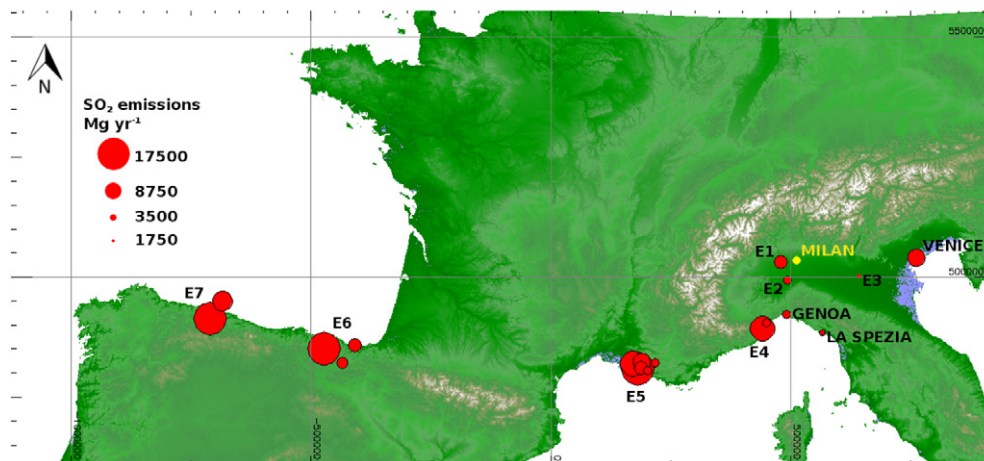


Fig. 4. Annual SO_2 emissions from point sources which potentially impacted on sulphur dioxide and sulphate ambient concentration in Milan in summer 2012. Source: DEM provided by Jarvis et al. (2008)

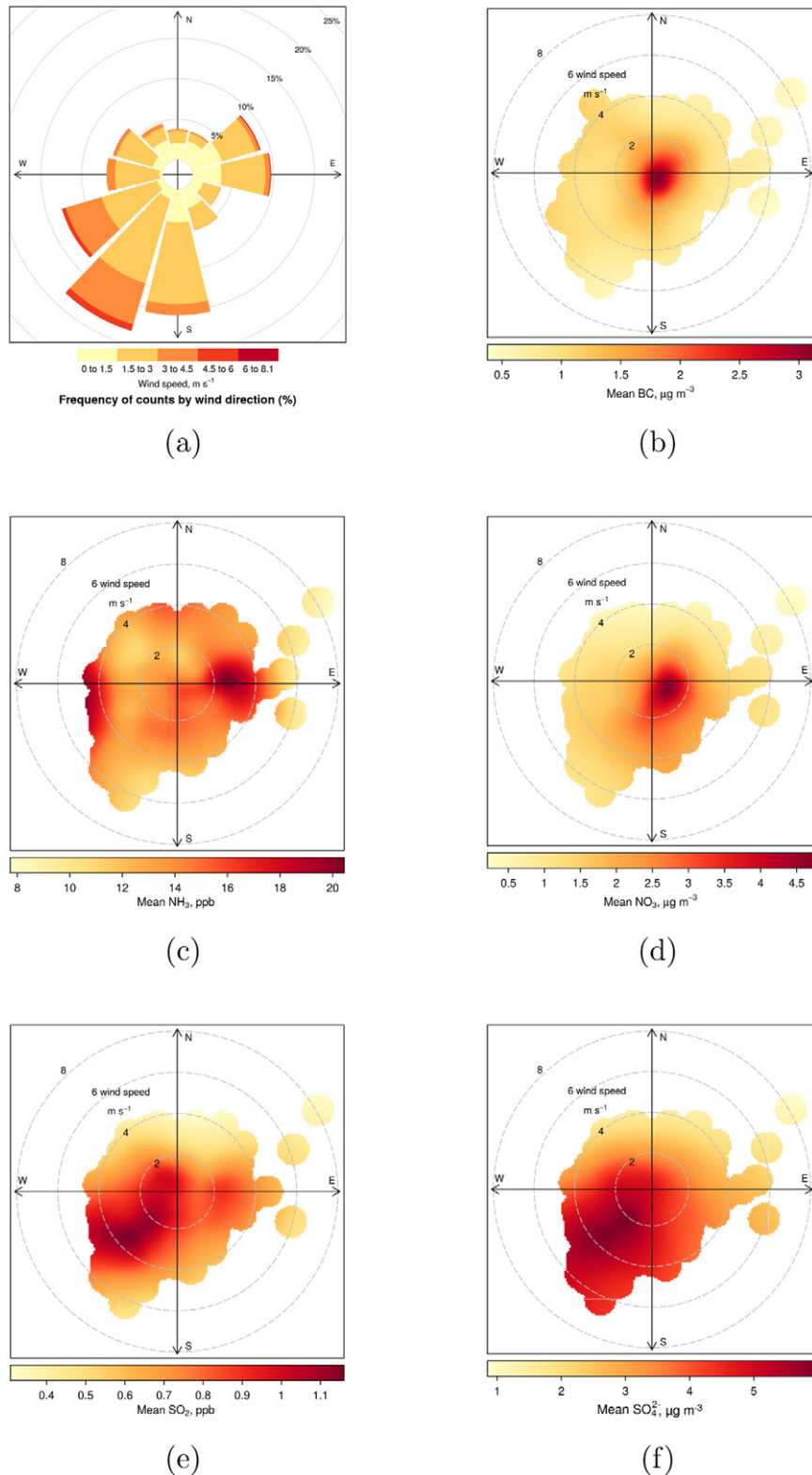


Fig. 5. Wind rose and bivariate polar plot of BC_E , NH_3 , NO_3^- , SO_2 and SO_4^{2-} ; colour codes correspond to concentration for each direction; circles correspond to wind speed.

transport from closer sources, within 36 h of travel distance: SO_2 oxidation rate for coal-fired power plant plume in summer was estimated as $\sim 1\% \text{h}^{-1}$ (Richards et al., 1981). Therefore the presence of other (e.g. more distant) sources of sulphate impacting Milan is

possible, although their identification would require backtrajectories longer than 36 h, better if associated to a particle dispersion model in order to provide reliable results for a BSMS (Han et al., 2005, e.g.) and beyond the aims of this study.

3.7. Elemental, organic and black carbon

EC exhibits a typical diurnal pattern of primary pollutants on weekdays, with a peak at 0800 CEST and a minimum when atmospheric mixing is highest. OC diurnal pattern on weekdays is featured by a slight afternoon increase due to secondary aerosol formation. The diurnal pattern for OC/EC ratio during weekdays, an index of secondary organic carbon formation, shows a minimum during primary emissions and a maximum during intense photochemical activity. No EC and OC data are available for Sundays. Following the rationale of Cabada et al. (2004), the EC tracer method was used to estimate secondary-influenced and primary-dominated OC, OC_s and OC_p respectively. Hours with lower photochemical activity were selected upon ozone levels: for each day the 25th quantile of Ozone was computed and only OC EC data during hours with Ozone below this threshold have been used to estimate the OC_p to EC regression. Some limitations apply to this simplistic rationale for the Po valley, where large levels of SOA are expected even at low ozone concentration. The primary-dominated OC to EC linear fit resulted in a slope of 1.7 and an intercept of $2.9\mu\text{g m}^{-3}$ (Fig. 6), similarly to the ratio of 1.7 found by Lonati et al. (2007) for summer 2002 and 2003 on daily $PM_{2.5}$ samples in Milan. The intercept most likely includes sampling artefacts, non-combustion OC emissions (e.g. biogenic), meatcooking operations and background OC. These coefficients were used to estimate secondary organic aerosol (SOA) concentration and finally CBPF was used to estimate potential transport. Results show how peak SOA values are associated to winds from the SW sector, i.e. to afternoon winds with maximum solar radiation and photochemical activity. Median concentration of SOA are associated to Easterly winds, most likely transported from OC emissions within the Po valley.

Absorption coefficient by MAAP is well correlated to EC, leading to an average mass absorption coefficient $MAC = 13.8 \pm 0.2\text{m}^2\text{g}^{-1}$, in

fair agreement to previous studies on off-line quartz fibre filters sampled in Milan (Vecchi et al., 2012). MAC is fairly constant throughout the day, with a daytime $MAC_{\text{day}} = 13.5 \pm 0.3\text{m}^2\text{g}^{-1}$ and nighttime $MAC_{\text{night}} = 13.9 \pm 0.3\text{m}^2\text{g}^{-1}$ (Fig. S13), indicating the same EC source, most likely traffic.

BC_E and EC, along with nitric oxide, show similar bivariate polar plots indicating a nearby main source sited SSE, along the direction of the nearest major road (see Fig. 5b for BC_E). CBPF associates lower concentration in BC_E and EC to SW winds, because of the dispersion induced by the stronger SW afternoon winds.

4. Conclusions

The article presented the most recent and complete analysis of 1-hour resolution observations of gaseous pollutants and main chemical composition of $PM_{2.5}$ in Milan. Ozone and nitrogen oxides pattern are consistent with intense photochemical activity under strong solar radiation, heavy emission sources and recirculation of pollutants, along with re-entrainment from the residual layer. HONO mixing ratios, compared to 1998, exhibited a decrease, consistently with the reduction in NO_2 atmospheric concentration, although with a similar formation rate. Particulate nitrate formed through two pathways, depending upon the meteorological conditions and air mass origin. Backtrajectories and pollution rose models attributed sulphur dioxide and sulphate in Milan to emission sources in the Po valley, in the Ligurian coast and Ligurian sea. Steady high levels of ammonia have been observed throughout the campaign, originated mostly by agricultural emissions within the whole Po valley. A distinct pattern was observed for hydrochloric acid: several potential sources were investigated and results hints to evaporation of a chlorinated compound, although further studies are needed to provide a clear answer.

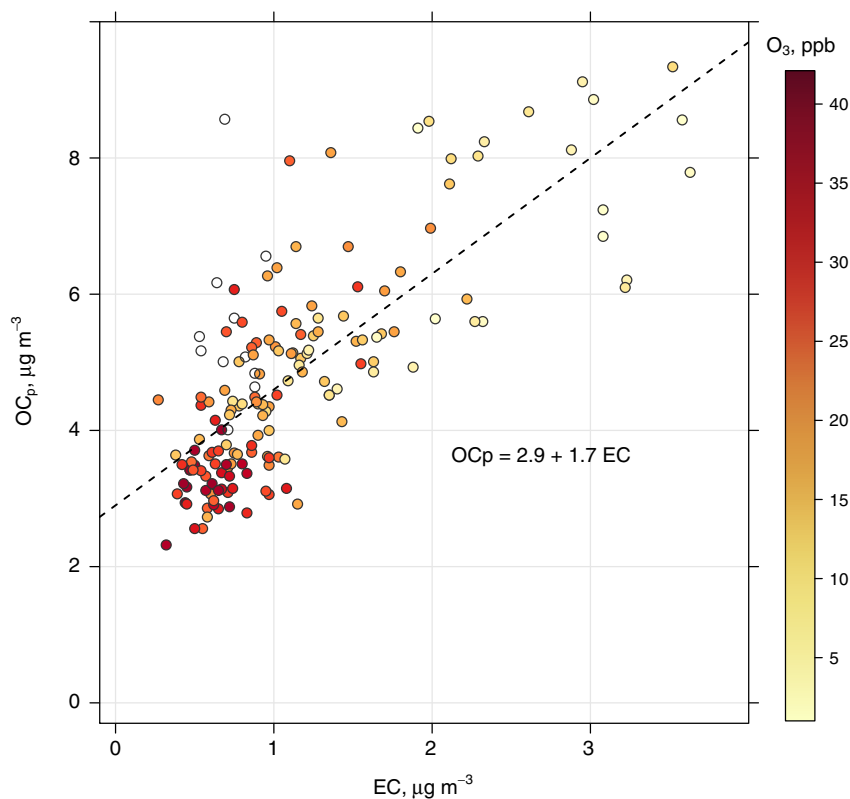


Fig. 6. Scatter plot of primary-dominated OC (OC_p) vs EC data, colour-coded according to O_3 levels. Dashed line represents the linear regression model fit for the estimate of the OC_p/EC ratio.

The atmospheric stability conditions enduring during the campaign allowed to investigate in details processing and ageing of several gas phase and aerosol pollutants. Overall variability has been checked by hierarchical cluster analysis, with a distance matrix based on Pearson's correlation coefficient (Bigi and Ghermandi, 2014) and grouping driven by a divisive algorithm (Kaufman and Rousseeuw, 1990). Results showed a strong correlation among most pollutants and a modest cluster structure, featured by two groups (Fig. S14): the first group includes long range transported pollutants (e.g. SO₂, SO₄²⁻) and compounds strongly correlated to radiation and temperature. The second group includes locally emitted and locally formed pollutants, e.g. BC and NO₃⁻. Implications of these results for local air quality policies are several: a large metropolitan area, although sited in a confined valley and under long-lasting atmospheric stability, can have air quality significantly affected by long-range transported pollutants. Moreover concentration variability of locally emitted pollutants in this same metropolitan area relies on the variability of overall emissions within the valley, therefore more attention needs to be paid to wide emissions, e.g. organic aerosol and ammonia. Conventional air quality policies aim to decrease concentration of regulatory pollutants (e.g. NO₂): we showed how their outcome controls the variation of less frequently monitored pollutants (e.g. HONO), whose influence on local air quality and climate is large and neglected by policymakers. Po valley plume stretches towards several European regions surrounding Italy on the East and South (Finardi et al., 2014), including large parts of the Mediterranean sea, contributing to acidification and eutrophication (Jalkanen et al., 2000; Im et al., 2013). Study outlooks include a source apportionment analysis and deeper investigation of carbonaceous aerosol and secondary organic formation events.

Acknowledgments

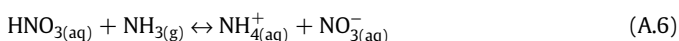
Thanks to Luca Lombroso for the description of the synoptic meteorological conditions.

Appendix A. Nitrate formation pathways

Formation of nitrate through homogeneous reaction pathway



Formation of nitrate through heterogeneous reaction pathway with nighttime formation of nitrate radical NO₃, its reaction to dinitrogen pentoxide N₂O₅, the hydrolysis of N₂O₅ on surfaces releasing HNO_{3(aq)} which is finally hydrolysed to nitrate, similarly to the reaction (A.2).



Appendix B. Calculation of equilibrium constants for ammonium nitrate

K_p and K_p^{*} are the dissociation constants for solid phase and aqueous ammonium nitrate respectively, estimated according to Mozurkewich (1993). K_{AN} is the equilibrium constant for reaction (A.2), estimated according to Seinfeld and Pandis (2006) and Poulain et al. (2011).

Deliquescence relative humidity for ammonium nitrate (Seinfeld and Pandis, 2006):

$$\ln(\text{DRH}) = \frac{723.7}{T} + 1.6954 \quad (\text{B.1})$$

Dissociation constant K_p for solid ammonium nitrate formed through reaction (A.2) (Mozurkewich, 1993):

$$\ln(K_p) = 118.87 - \frac{24084}{T} - 6.025 \ln(T) \quad (\text{B.2})$$

Dissociation constant K_p^{*} for aqueous ammonium nitrate formed through reaction (A.2) (Mozurkewich, 1993):

$$K_p^* = (P_1 - P_2(1 - a_w) + P_3(1 - a_w)^2) \cdot (1 - a_w)^{1.75} \cdot K_p \quad (\text{B.3})$$

with

$$\ln(P_1) = -135.94 + \frac{8763}{T} + 19.12 \ln(T) \quad (\text{B.4})$$

$$\ln(P_2) = -122.65 + \frac{9969}{T} + 16.22 \ln(T) \quad (\text{B.5})$$

$$\ln(P_3) = -182.61 + \frac{13875}{T} + 24.46 \ln(T) \quad (\text{B.6})$$

and water activity *a_w* approximated by RH expressed in the range of 0–1.

Table B1

Statistical values of gas, particles and meteorological parameters during the whole campaign. Note: for global radiation the range of maximum diurnal is indicated; for precipitation the total rainfall and the maximum intensity are indicated.

Parameter	Mean ±σ	Median
Nitric oxide (NO), ppb	4.58 ± 2.66	4.00
Nitrogen dioxide (NO ₂), ppb	6.41 ± 6.46	4.18
Nitrogen oxides as NO ₂ (NO _x), ppb	10.99 ± 8.10	8.00
Ozone (O ₃), ppb	41.73 ± 19.73	41.10
Organic carbon (OC), μgm ⁻³	6.16 ± 4.53	4.42
Elemental carbon (EC), μgm ⁻³	0.70 ± 0.61	0.62
Equivalent black carbon (BC _E), μgm ⁻³	1.59 ± 1.16	1.25
Hydrochloric acid (HCl), ppb	0.19 ± 0.20	0.12
Ammonia (NH ₃), ppb	14.40 ± 5.25	13.18
Nitrous acid (HONO), ppb	0.55 ± 0.34	0.49
Nitric acid (HNO ₃), ppb	0.71 ± 0.51	0.60
Sulphur dioxide (SO ₂), ppb	0.92 ± 0.50	0.79
Calcium ion (Ca ²⁺), μgm ⁻³	0.27 ± 0.21	0.20
Chloride ion (Cl ⁻), μgm ⁻³	0.10 ± 0.21	0.10
Potassium ion (K ⁺), μgm ⁻³	0.08 ± 0.18	0.10
Magnesium ion (Mg ²⁺), μgm ⁻³	0.04 ± 0.10	0.00
Sodium ion (Na ⁺), μgm ⁻³	0.67 ± 0.79	0.30
Ammonium ion (NH ₄ ⁺), μgm ⁻³	5.63 ± 3.40	5.00
Nitrite ion (NO ₂ ⁻), μgm ⁻³	1.01 ± 0.58	0.90
Nitrate ion (NO ₃ ⁻), μgm ⁻³	2.72 ± 3.15	1.80
Sulphate ion (SO ₄ ²⁻), μgm ⁻³	4.82 ± 2.22	4.60
Atmospheric pressure (p), hPa	996.6 ± 3.9	996.3
Atmospheric temperature (T), °C	26.0 ± 4.5	25.8
Global radiation (GR), Wm ⁻²	396.20–909.67	
Precipitation (r) ^a , mm–mmh ⁻¹	134.8–29.4	
Radon (Rn), Bqm ⁻³	6.1 ± 4.0	4.8
Relative humidity (RH), %	51.9 ± 16.0	50.4
Wind speed (W), ms ⁻¹	1.2 ± 0.9	1.1

Equilibrium constant K_{AN} of ammonium nitrate at RH above that of deliquescence ammonium nitrate, in ppb^2 from Poulain et al. (2011).

$$K_{AN} = k(298) \exp \left\{ a \left(\frac{298}{T} - 1 \right) + b \left[1 + \ln \left(\frac{298}{T} \right) - \frac{298}{T} \right] \right\} \cdot 10^{-18} \quad (\text{B.7})$$

with $k(298) = 3.35 \cdot 10^{-16}$, atm^{-2} , $a = 75.11$, $b = -13.5$

Appendix C. Supplementary figures

Supplementary data to this article can be found online at <http://dx.doi.org/10.1016/j.atmosres.2016.10.025>.

References

- Acker, K., Möller, D., Auel, R., Wieprecht, W., Kalaß, D., 2005. Concentrations of nitrous acid, nitric acid, nitrite and nitrate in the gas and aerosol phase at a site in the emission zone during ESCOMPTE 2001 experiment. *Atmos. Res.* 74, 507–524. <http://dx.doi.org/10.1016/j.atmosres.2004.04.009>.
- AERA, 2015. OGC-WMS Server. Last access: 2015-01-07. http://geomap.reteunitaria.piemonte.it/ws/aera/rp-01/aerawms/wms_aera_emissioni_tot?
- Alexander, B., Hastings, M.G., Allman, D.J., Dachs, J., Thornton, J.A., Kunasek, S.A., 2009. Quantifying atmospheric nitrate formation pathways based on a global model of the oxygen isotopic composition ($\delta^{17}\text{O}$) of atmospheric nitrate. *Atmos. Chem. Phys.* 9, 5043–5056. <http://dx.doi.org/10.5194/acp-9-5043-2009>.
- Alicke, B., Platt, U., Stutz, J., 2002. Impact of nitrous acid photolysis on the total hydroxyl radical budget during the limitation of oxidant production/pianura padana produzione di ozono study in Milan. *J. Geophys. Res.: Atmos.* 107, 8196. <http://dx.doi.org/10.1029/2000JD000075>.
- Bae, M.-S., Schauer, J.J., DeMinter, J.T., Turner, J.R., Smith, D., Cary, R.A., 2004. Validation of a semi-continuous instrument for elemental carbon and organic carbon using a thermal-optical method. *Atmos. Environ.* 38, 2885–2893. <http://dx.doi.org/10.1016/j.atmosenv.2004.02.027>.
- Baltensperger, U., Streit, N., Weingartner, E., Nyeki, S., Prévôt, A.S.H., Van Dingenen, R., Virkkula, A., Putaud, J.-P., Even, A., ten Brink, H., Blatter, A., Gäggeler, H.W., 2002. Urban and rural aerosol characterization of summer smog events during the PIPAPO field campaign in Milan, Italy. *J. Geophys. Res.* D107, 8193. <http://dx.doi.org/10.1029/2001JD001292>.
- Bari, A., Ferraro, V., Wilson, L.R., Luttinger, D., Husain, L., 2003. Measurements of gaseous HONO, HNO_3 , SO_2 , HCl, NH_3 , particulate sulfate and $\text{PM}_{2.5}$ in New York, NY. *Atmos. Environ.* 37, 2825–2835. [http://dx.doi.org/10.1016/S1352-2310\(03\)00199-7](http://dx.doi.org/10.1016/S1352-2310(03)00199-7).
- Bernardoni, V., Vecchi, R., Valli, G., Piazzalunga, A., Fermo, P., 2011. PM_{10} source apportionment in Milan (Italy) using time-resolved data. *Science of The Total Environment* 409, 4788–4795. <http://dx.doi.org/10.1016/j.scitotenv.2011.07.048>.
- Bigi, A., Ghermandi, G., 2014. Long-term trend and variability of atmospheric PM_{10} concentration in the Po Valley. *Atmos. Chem. Phys.* 14, 4895–4907. <http://dx.doi.org/10.5194/acp-14-4895-2014>.
- Bigi, A., Ghermandi, G., 2016. Trends and variability of atmospheric $\text{PM}_{2.5}$ and $\text{PM}_{10-2.5}$ concentration in the Po Valley, Italy. *Atmos. Chem. Phys. Discuss.* 2016, 1–19. <http://dx.doi.org/10.5194/acp-2016-441>.
- Bigi, A., Ghermandi, G., Harrison, R.M., 2012. Analysis of the air pollution climate at a background site in the Po valley. *J. Environ. Monit.* 14, 552–563. <http://dx.doi.org/10.1039/c1em10728c>.
- Cabada, J., Pandis, S., Subramanian, R., Robinson, A., Polidori, A., Turpin, B., Cabada, J., Pandis, S., Subramanian, R., Robinson, A., Polidori, A., Turpin, B., 2004. Estimating the secondary organic aerosol contribution to $\text{PM}_{2.5}$ using the EC tracer method. *Aerosol Sci. Tech.* 38, 140–155. <http://dx.doi.org/10.1080/02786820390229084>.
- Carslaw, D., Ropkins, K., 2012. Openair - an R package for air quality data analysis. *Environ. Model. Softw.* 27–28, 52–61.
- Cavalli, F., Viana, M., Yttri, K.E., Genberg, J., Putaud, J.-P., 2010. Toward a standardized thermal-optical protocol for measuring atmospheric organic and elemental carbon: the EUSAAR protocol. *Atmos. Meas. Tech.* 3, 79–89. <http://dx.doi.org/10.5194/amt-3-79-2010>.
- Cleveland, W.S., Graedel, T.E., Kleiner, B., Warner, J.L., 1974. Sunday and workday variations in photochemical air pollutants in New Jersey and New York. *Science* 186, 1037–1038. <http://dx.doi.org/10.1126/science.186.4168.1037>.
- Denier van der Gon, H. A. C., Curci, G., Ferrero, L., Tuccella, P., Barnaba, F., Angelini, F., Bolzacchini, E., Carbone, C., Facchini, M.C., Gobbi, G.P., Kuenen, J.P.P., Landi, T.C., Perrino, C., Perrone, M.G., Sangiorgi, G., Stocchi, P., 2015. How much is particulate matter near the ground influenced by upper-level processes within and above the PBL? A summertime case study in Milan (Italy) evidences the distinctive role of nitrate. *Atmos. Chem. Phys.* 15, 2629–2649. <http://dx.doi.org/10.5194/acp-15-2629-2015>.
- D'Alessandro, A., Lucarelli, F., Mandò, P., Marcazzan, G., Nava, S., Prati, P., Valli, G., Vecchi, R., Zucchiatti, A., 2003. Hourly elemental composition and sources identification of fine and coarse PM_{10} particulate matter in four Italian towns. *J. Aerosol Sci.* 34, 243–259. [http://dx.doi.org/10.1016/S0021-8502\(02\)00172-6](http://dx.doi.org/10.1016/S0021-8502(02)00172-6).
- D'Alessandro, A., Lucarelli, F., Marcazzan, G., Nava, S., Prati, P., Valli, G., Vecchi, R., Zucchiatti, A., 2004. A summertime investigation on urban PM fine and coarse fractions using hourly elemental concentration data series. *Nuovo Cimento Soc. Ital. Fis., C 27*, 17–28. <http://dx.doi.org/10.1393/ncc/i2003-10015-7>.
- Draxler, R., Rolph, G., 2013. HYSPLIT (HYbrid single-particle lagrangian integrated trajectory). Model access via NOAA ARL READY Website. <http://www.arl.noaa.gov/HYSPLIT.php>.
- Eldering, A., Solomon, P.A., Salmon, L.G., Fall, T., Cass, G.R., 1991. Hydrochloric acid: a regional perspective on concentrations and formation in the atmosphere of Southern California. *Atmos. Environ. A. Gen. Top.* 25, 2091–2102. [http://dx.doi.org/10.1016/0960-1686\(91\)90086-M](http://dx.doi.org/10.1016/0960-1686(91)90086-M).
- Febo, A., Perrino, C., Allegrini, I., 1996. Measurement of nitrous acid in Milan, Italy, by DOAS and diffusion denuders. *Atmos. Environ.* 30, 3599–3609. [http://dx.doi.org/10.1016/1352-2310\(96\)00069-6](http://dx.doi.org/10.1016/1352-2310(96)00069-6).
- Finardi, S., Silibello, C., D'Allura, A., Radice, P., 2014. Analysis of pollutants exchange between the Po valley and the surrounding European region. *Urban Clim.* 10, Part 4, 682–702. <http://dx.doi.org/10.1016/j.uclim.2014.02.002>.
- Finlayson-Pitts, B.J., Pitts, J.N., 2000. *Chemistry of the Upper and Lower Atmosphere*. Academic Press, San Diego, USA., pp. 969.
- Fleming, Z.L., Monks, P.S., Manning, A.J., 2012. Review: untangling the influence of air-mass history in interpreting observed atmospheric composition. *Atmos. Res.* 104–105, 1–39. <http://dx.doi.org/10.1016/j.atmosres.2011.09.009>.
- Fountoukis, C., Nenes, A., 2007. ISORROPIA II: a computationally efficient thermodynamic equilibrium model for K^+ - Ca^{2+} - Mg^{2+} - NH_4^+ - Na^+ - SO_4^{2-} - NO_3^- - Cl^- - H_2O aerosols. *Atmos. Chem. Phys.* 7, 4639–4659. <http://dx.doi.org/10.5194/acp-7-4639-2007>.
- Gutzwiller, L., Arens, F., Baltensperger, U., Gäggeler, H.W., Ammann, M., 2002. Significance of semivolatile diesel exhaust organics for secondary HONO formation. *Environ. Sci. Technol.* 36, 677–682. <http://dx.doi.org/10.1021/es015673b>.
- Han, Y., Holsen, T., Hopke, P., Yi, S., 2005. Comparison between back-trajectory based modeling and Lagrangian backward dispersion modeling for locating sources of reactive gaseous mercury. *Environ. Sci. Technol.* 39, 1715–1723. <http://dx.doi.org/10.1021/es0498540>.
- Henschel, S., Querol, X., Atkinson, R., Pandolfi, M., Zeka, A., Tertre, A.L., Analitis, A., Katsouyanni, K., Chanel, O., Pascal, M., Boudand, C., Haluz, D., Medina, S., Goodman, P.G., 2013. Ambient air SO_2 patterns in 6 European cities. *Atmos. Environ.* 79, 236–247. <http://dx.doi.org/10.1016/j.atmosenv.2013.06.008>.
- Im, U., Christodoulou, S., Violaki, K., Zampas, P., Kocak, M., Daskalakis, N., Mihalopoulos, N., Kanakidou, M., 2013. Atmospheric deposition of nitrogen and sulfur over southern Europe with focus on the mediterranean and the black sea. *Atmos. Environ.* 81, 660–670. <http://dx.doi.org/10.1016/j.atmosenv.2013.09.048>.
- INEMAR, 2015. Last access: 2015-01-07. <http://www.inemar.eu>.
- Jalkanen, L., Mäkinen, A., Häsänen, E., Juhanoja, J., 2000. The effect of large anthropogenic particulate emissions on atmospheric aerosols, deposition and bioindicators in the Eastern Gulf of Finland region. *Sci. Total Environ.* 262, 123–136. [http://dx.doi.org/10.1016/S0048-9697\(00\)00602-1](http://dx.doi.org/10.1016/S0048-9697(00)00602-1).
- Jarvis, A., Reuter, H.I., Nelson, A., Guevara, E., 2008. Hole-filled seamless SRTM data v4. Tech. rep., International Centre for Tropical Agriculture (CIAT), <http://srtm.csi.cgiar.org>.
- Jiménez, P., Parra, R., Gassó, S., Baldasano, J.M., 2005. Modeling the ozone weekend effect in very complex terrains: a case study in the northeastern Iberian peninsula. *Atmos. Environ.* 39, 429–444. <http://dx.doi.org/10.1016/j.atmosenv.2004.09.065>.
- Jung, J., Kim, Y.J., Lee, K.Y., Kawamura, K., Hu, M., Kondo, Y., 2011. The effects of accumulated refractory particles and the peak inert mode temperature on semi-continuous organic carbon and elemental carbon measurements during the CAREBeijing 2006 campaign. *Atmos. Environ.* 45, 7192–7200. <http://dx.doi.org/10.1016/j.atmosenv.2011.09.003>.
- Kalberer, M., Ammann, M., Arens, F., Gäggeler, H.W., Baltensperger, U., 1999. Heterogeneous formation of nitrous acid (HONO) on soot aerosol particles. *J. Geophys. Res. Atmos.* 104, 13825–13832. <http://dx.doi.org/10.1029/1999JD900141>.
- Kaneyasu, N., Yoshikado, H., Mizuno, T., Sakamoto, K., Soufuku, M., 1999. Chemical forms and sources of extremely high nitrate and chloride in winter aerosol pollution in the Kanto plain of Japan. *Atmos. Environ.* 33, 1745–1756. [http://dx.doi.org/10.1016/S1352-2310\(98\)00396-3](http://dx.doi.org/10.1016/S1352-2310(98)00396-3).
- Kaufman, L., Rousseeuw, P.J., 1990. *Finding Groups in Data: An Introduction to Cluster Analysis*. Wiley, New York.
- Kleffmann, J., 2007. Daytime sources of nitrous acid (HONO) in the atmospheric boundary layer. *ChemPhysChem* 8, 1137–1144. <http://dx.doi.org/10.1002/cphc.200700016>.
- Kleffmann, J., Lörzer, J., Wiesen, P., Kern, C., Trick, S., Volkamer, R., Rodenas, M., Wirtz, K., 2006. Intercomparison of the DOAS and LOPAP techniques for the detection of nitrous acid (HONO). *Atmos. Environ.* 40, 3640–3652. <http://dx.doi.org/10.1016/j.atmosenv.2006.03.027>.
- Kurtenbach, R., Becker, K., Gomes, J., Kleffmann, J., Lörzer, J., Spittler, M., Wiesen, P., Ackermann, R., Geyer, A., Platt, U., 2001. Investigations of emissions and heterogeneous formation of HONO in a road traffic tunnel. *Atmos. Environ.* 35, 3385–3394. [http://dx.doi.org/10.1016/S1352-2310\(01\)00138-8](http://dx.doi.org/10.1016/S1352-2310(01)00138-8).
- Lammel, G., Cape, J.N., 1996. Nitrous acid and nitrite in the atmosphere. *Chem. Soc. Rev.* 25, 361–369. <http://dx.doi.org/10.1039/CS9962500361>.

- Lightowers, P., Cape, J., 1988. Sources and fate of atmospheric HCl in the U.K. and Western Europe. *Atmos. Environ.* (1967) 22, 7–15. [http://dx.doi.org/10.1016/0004-6981\(88\)90294-6](http://dx.doi.org/10.1016/0004-6981(88)90294-6).
- Lonati, G., Ozgen, S., Giugliano, M., 2007. Primary and secondary carbonaceous species in PM_{2.5} samples in Milan (Italy). *Atmos. Environ.* 41, 4599–4610. <http://dx.doi.org/10.1016/j.atmosenv.2007.03.046>.
- Marcazzan, G., Caprioli, E., Valli, G., Vecchi, R., 2003. Temporal variation of ²¹²Pb concentration in outdoor air of Milan and a comparison with ²¹⁴Bi. *J. Environ. Radioact.* 65, 77–90. [http://dx.doi.org/10.1016/S0265-931X\(02\)00089-9](http://dx.doi.org/10.1016/S0265-931X(02)00089-9).
- Markovic, M.Z., VandenBoer, T.C., Murphy, J.G., 2012. Characterization and optimization of an online system for the simultaneous measurement of atmospheric water-soluble constituents in the gas and particle phases. *J. Environ. Monit.* 14, 1872–1884. <http://dx.doi.org/10.1039/C2EM00004K>.
- Michalski, G., Scott, Z., Kabling, M., Thiemens, M.H., 2003. First measurements and modeling of $\delta^{17}\text{O}$ in atmospheric nitrate. *Geophys. Res. Lett.* 30, <http://dx.doi.org/10.1029/2003GL017015>.
- Michoud, V., Colomb, A., Borbon, A., Miet, K., Beekmann, M., Camredon, M., Aumont, B., Perrier, S., Zapf, P., Siour, G., Ait-Helal, W., Affif, C., Kukui, A., Furger, M., Dupont, J.C., Haefelin, M., Doussin, J.F., 2014. Study of the unknown HONO daytime source at a European suburban site during the MEGAPOLI summer and winter field campaigns. *Atmos. Chem. Phys.* 14, 2805–2822. <http://dx.doi.org/10.5194/acp-14-2805-2014>.
- Mozurkewich, M., 1993. The dissociation constant of ammonium nitrate and its dependence on temperature, relative humidity and particle size. *Atmos. Environ.* A. Gen. Top. 27, 261–270. [http://dx.doi.org/10.1016/0960-1686\(93\)90356-4](http://dx.doi.org/10.1016/0960-1686(93)90356-4).
- Nefel, A., Spirig, C., Prévôt, A.S.H., Furger, M., Stutz, J., Vogel, B., Hjorth, J., 2002. Sensitivity of photooxidant production in the Milan basin: an overview of results from a EUROTRAC-2 limitation of oxidant production field experiment. *Journal of Geophysical Research: Atmospheres* 107, 8188. <http://dx.doi.org/10.1029/2001JD001263>.
- Penkett, S., Jones, B., Brich, K., Eggleton, A., 1979. The importance of atmospheric ozone and hydrogen peroxide in oxidising sulphur dioxide in cloud and rainwater. *Atmospheric Environment* (1967) 13, 123–137. [http://dx.doi.org/10.1016/0004-6981\(79\)90251-8](http://dx.doi.org/10.1016/0004-6981(79)90251-8).
- Perrone, M., Larsen, B., Ferrero, L., Sangiorgi, G., Gennaro, G.D., Udisti, R., Zangrando, R., Gambaro, A., Bolzacchini, E., 2012. Sources of high PM_{2.5} concentrations in Milan, northern Italy: molecular marker data and CMB modelling. *Sci. Total Environ.* 414, 343–355. <http://dx.doi.org/10.1016/j.scitotenv.2011.11.026>.
- Petzold, A., Kramer, H., Schönlinner, M., 2002. Continuous measurement of atmospheric black carbon using a multi-angle absorption photometer. *Environ. Sci. Pollut. Res.* 4, 78–82.
- Pollack, I., Ryerson, T., Trainer, M., Parrish, D., Andrews, A., Atlas, E., Blake, D., Brown, S., Commane, R., Daube, B., De Gouw, J., Dubé, W., Flynn, J., Frost, G., Gilman, J., Grossberg, N., Holloway, J., Kofler, J., Kort, E., Kuster, W., Lang, P., Lefer, B., Lueb, R., Neuman, J., Nowak, J., Novelli, P., Peischl, J., Perring, A., Roberts, J., Santoni, G., Schwarz, J., Spackman, J., Wagner, N., Warneke, C., Washenfelder, R., Wofsy, S., Xiang, B., 2012. Airborne and ground-based observations of a weekend effect in ozone, precursors, and oxidation products in the California south coast air basin. *J. Geophys. Res. Atmos.* 117, <http://dx.doi.org/10.1029/2011JD016772>.
- Poulain, L., Spindler, G., Birmili, W., Plass-Dülmer, C., Wiedensohler, A., Herrmann, H., 2011. Seasonal and diurnal variations of particulate nitrate and organic matter at the IFT research station Melpitz. *Atmos. Chem. Phys.* 11, 12579–12599. <http://dx.doi.org/10.5194/acp-11-12579-2011>.
- Putaud, J.-P., Van Dingenen, R., Alastuey, A., Bauer, H., Birmili, W., Cyrys, J., Flentje, H., Fuzzi, S., Gehrig, R., Hansson, H.C., Harrison, R.M., Herrmann, H., Hitznerberger, R., Hüglin, C., Jones, A.M., Kasper-Giebl, A., Kiss, G., Kouss, A., Kuhlbusch, T.A.J., Löschau, G., Maenhaut, W., Molnar, A., Moreno, T., Pekkanen, J., Perrino, C., Pitz, M., Puxbaum, H., Querol, X., Rodriguez, S., Salma, I., Schwarz, J., Smolik, J., Schneider, J., Spindler, G., ten Brink, H., Tursic, J., Viana, M., Wiedensohler, A., Raes, F., 2010. A European aerosol phenomenology - 3: physical and chemical characteristics of particulate matter from 60 rural, urban, and kerbside sites across Europe. *Atmos. Environ.* 44, 1308–1320. <http://dx.doi.org/10.1016/j.atmosenv.2009.12.011>.
- Putaud, J.-P., Van Dingenen, R., Raes, F., 2002. Submicron aerosol mass balance at urban and semirural sites in the Milan area (Italy). *J. Geophys. Res. Atmos.* 107, 8198. <http://dx.doi.org/10.1029/2000JD000111>.
- Core Team, R., 2013. *R: A Language and Environment for Statistical Computing*. R Foundation for Statistical Computing, Vienna, Austria.
- Ravishankara, A.R., 1997. Heterogeneous and multiphase chemistry in the troposphere. *Science* 276, 1058–1065. <http://dx.doi.org/10.1126/science.276.5315.1058>.
- Richards, L., Anderson, J., Blumenthal, D., Brandt, A., McDonald, J., Waters, N., Macias, E., Bhardwaj, P., 1981. Plumes and visibility measurements and model components the chemistry, aerosol physics, and optical properties of a western coal-fired power plant plume. *Atmos. Environ.* 15, 2111–2134. [http://dx.doi.org/10.1016/0004-6981\(81\)90245-6](http://dx.doi.org/10.1016/0004-6981(81)90245-6).
- Scheifinger, H., Kaiser, A., 2007. Validation of trajectory statistical methods. *Atmos. Environ.* 41, 8846–8856. <http://dx.doi.org/10.1016/j.atmosenv.2007.08.034>.
- Seinfeld, J.H., Pandis, S.N., 2006. *Atmospheric Chemistry and Physics*. 2nd edn. Wiley.
- Spindler, G., Hesper, J., Brüggemann, E., Dubois, R., Müller, T., Herrmann, H., 2003. Wet annular denuder measurements of nitrous acid: laboratory study of the artefact reaction of NO₂ with S(IV) in aqueous solution and comparison with field measurements. *Atmos. Environ.* 37, 2643–2662. [http://dx.doi.org/10.1016/S1352-2310\(03\)00209-7](http://dx.doi.org/10.1016/S1352-2310(03)00209-7).
- Stutz, J., Alicke, B., Nefel, A., 2002. Nitrous acid formation in the urban atmosphere: gradient measurements of NO₂ and HONO over grass in Milan, Italy. *J. Geophys. Res. Atmos.* 107, <http://dx.doi.org/10.1029/2001JD000390>.
- Tonse, S., Brown, N., Harley, R., Jin, L., 2008. A process-analysis based study of the ozone weekend effect. *Atmos. Environ.* 42, 7728–7736. <http://dx.doi.org/10.1016/j.atmosenv.2008.05.061>.
- Uria-Tellaetxe, I., Carslaw, D.C., 2014. Conditional bivariate probability function for source identification. *Environ. Model Softw.* 59, 1–9. <http://dx.doi.org/10.1016/j.envsoft.2014.05.002>.
- Vecchi, R., Valli, G., 1999. Ozone assessment in the southern part of the alps. *Atmos. Environ.* 33, 97–109. [http://dx.doi.org/10.1016/S1352-2310\(98\)00133-2](http://dx.doi.org/10.1016/S1352-2310(98)00133-2).
- Vecchi, R., Valli, G., Bernardoni, V., Paganelli, C., Piazzalunga, A., 2012. 2–7 September. Insights on BC determination on quartz-fibre and PTFE filters: results of two field experiments in Milan (Italy). In: Alados-Arboledas, L., Olmo Reyes, F.J. (Eds.), *Proceedings of the European Aerosol Conference 2012*. AWG08S1P17, European Aerosol Assembly, Granada, Spain.
- Vecchi, R., Valli, G., Fermo, P., D'Alessandro, A., Piazzalunga, A., Bernardoni, V., 2009. Organic and inorganic sampling artefacts assessment. *Atmos. Environ.* 43, 1713–1720. <http://dx.doi.org/10.1016/j.atmosenv.2008.12.016>.
- Wang, Y., Hu, B., Ji, D., Liu, Z., Tang, G., Xin, J., Zhang, H., Song, T., Wang, L., Gao, W., Wang, X., Wang, Y., 2014. Ozone weekend effects in the Beijing-Tianjin-Hebei metropolitan area, China. *Atmos. Chem. Phys.* 14, 2419–2429. <http://dx.doi.org/10.5194/acp-14-2419-2014>.
- Wood, S., 2006. *Generalized Additive Models: An Introduction with R*. Chapman & Hall/CRC, Boca Raton, USA.
- World Health Organization, 2006. *Air quality guidelines. Global update 2005*. Particulate matter, ozone, nitrogen dioxide and sulfur dioxide. World Health Organization, regional office for Europe, Copenhagen, Denmark.
- Zhang, J., Trivikrama Rao, S., 1999, dec. The role of vertical mixing in the temporal evolution of ground-level ozone concentrations. *J. Appl. Meteorol.* 38, 1674–1691. [http://dx.doi.org/10.1175/1520-0450\(1999\)038<i>iexcl;1674:TROVMI¿2.0.CO;2](http://dx.doi.org/10.1175/1520-0450(1999)038<i>iexcl;1674:TROVMI¿2.0.CO;2).
- Ziemba, L.D., Dibb, J.E., Griffin, R.J., Anderson, C.H., Whitlow, S.I., Lefer, B.L., Rappenglück, B., Flynn, J., 2010. Heterogeneous conversion of nitric acid to nitrous acid on the surface of primary organic aerosol in an urban atmosphere. *Atmos. Environ.* 44, 4081–4089. <http://dx.doi.org/10.1016/j.atmosenv.2008.12.024>.